ARGX-119 is an agonist antibody for human MuSK that reverses disease relapse in a mouse model of congenital myasthenic syndrome

Vanhauwaert, R.; Oury, J.; Vankerckhoven, B.; Steyaert, C.; Jensen, S.M.; Vergoossen, D.L.E.; ... ; Burden, S.J.

NEUROMUSCULAR DISEASE

ARGX-119 is an agonist antibody for human MuSK that reverses disease relapse in a mouse model of congenital myasthenic syndrome

Roeland Vanhauwaert[1]*†, Julien Oury[2]†, Bernhardt Vankerckhoven[1], Christophe Steyaert[1], Stine Marie Jensen[3], Dana L. E. Vergoossen[3], Christa Kneip[1], Leah Santana[2], Jamie L. Lim[1,3], Jaap J. Plomp[4], Roy Augustinus[3], Shohei Koide[5,6], Christophe Blanchetot[1], Peter Ulrichts[1], Maartje G. Huijbers[3,4]‡, Karen Silence[1]‡, Steven J. Burden[2,7]*‡

Muscle-specific kinase (MuSK) is essential for the formation, function, and preservation of neuromuscular synapses. Activation of MuSK by a MuSK agonist antibody may stabilize or improve the function of the neuromuscular junction (NMJ) in patients with disorders of the NMJ, such as congenital myasthenia (CM). Here, we generated and characterized ARGX-119, a first-in-class humanized agonist monoclonal antibody specific for MuSK, that is being developed for treatment of patients with neuromuscular diseases. We performed in vitro ligand-binding assays to show that ARGX-119 binds with high affinity to the Frizzled-like domain of human, nonhuman primate, rat, and mouse MuSK, without off-target binding, making it suitable for clinical development. Within the Fc region, ARGX-119 harbors L234A and L235A mutations to diminish potential immune-activating effector functions. Its mode of action is to activate MuSK, without interfering with its natural ligand neural Agrin, and cluster acetylcholine receptors in a dose-dependent manner, thereby stabilizing neuromuscular function. In a mouse model of *DOK7* CM, ARGX-119 prevented early postnatal lethality and reversed disease relapse in adult *Dok7* CM mice by restoring neuromuscular function and reducing muscle weakness and fatigability in a dose-dependent manner. Pharmacokinetic studies in nonhuman primates, rats, and mice revealed a nonlinear PK behavior of ARGX-119, indicative of target-mediated drug disposition and in vivo target engagement. On the basis of this proof-of-concept study, ARGX-119 has the potential to alleviate neuromuscular diseases hallmarked by impaired neuromuscular synaptic function, warranting further clinical development.

INTRODUCTION

Diseases of the neuromuscular junction (NMJ) impair neuromuscular transmission, causing debilitating and potentially life-threatening muscle weakness. At the NMJ, motor nerve terminals release the neurotransmitter acetylcholine (ACh), which diffuses across the synaptic cleft and binds to ACh receptors (AChRs) in the muscle membrane. Binding of two ACh molecules opens the ligand-gated ion channel, depolarizing the muscle membrane and initiating an action potential that stimulates muscle contraction (*1*, *2*).

Muscle-specific kinase (MuSK) is a receptor tyrosine kinase essential for the establishment and preservation of the NMJ. MuSK is expressed and required throughout life (*1*, *3*–*5*), and defects in MuSK signaling are a cause of muscle weakness in congenital myasthenic syndrome (CMS) and myasthenia gravis (MG) (*6*). MuSK is a transmembrane protein composed of an extracellular region with three immunoglobulin-like domains (Ig-like domains 1 to 3), a Frizzled-like domain (Fz), a transmembrane domain, and an intracellular kinase domain (*7*, *8*). The motor neuron–derived heparan sulfate proteoglycan Agrin induces synaptic differentiation by binding low-density lipoprotein receptor–related protein 4 (LRP4), which promotes association between LRP4 and MuSK and stimulates MuSK tyrosine phosphorylation (*9*–*13*). MuSK phosphorylation leads to recruitment of downstream of kinase 7 (DOK7), essential for anchoring and clustering AChRs on the postsynaptic side of the NMJ, enabling neuromuscular transmission and muscle contraction (*7*, *14*, *15*). MuSK is also required for presynaptic differentiation (*3*), given that MuSK clusters LRP4, which signals back to motor neurons to stimulate differentiation of motor nerve terminals (*16*).

Agonist antibodies that bind the MuSK Fz-like domain and force-dimerize MuSK have shown preclinical therapeutic potential in models of amyotrophic lateral sclerosis (ALS) and congenital myasthenia (CM) (*17*–*19*). However, these antibodies either recognize proteins in addition to MuSK or fail to recognize human MuSK (*17*, *20*). Thus, discovery of a MuSK agonist antibody that binds selectively to MuSK in humans and mice would be an important step forward in clinical development of a therapeutic for treating neuromuscular diseases.

The MuSK Fz-like domain is attractive for antibody targeting because this domain is dispensable for MuSK function, and agonist antibodies that bind this domain are well tolerated in mice (*17*–*19*, *21*, *22*). Here, we describe the development of ARGX-119, a monoclonal antibody (mAb) targeting the MuSK Fz-like domain. We found that binding of ARGX-119 to the MuSK Fz-like domain facilitates dimerization of MuSK, initiating MuSK phosphorylation

[1]argenx , 9052 Zwijnaarde, Belgium. [2]Helen L. and Martin S. Kimmel Center for Biology and Medicine at Skirball Institute of Biomolecular Medicine, NYU School of Medicine, New York, NY 10016, USA. [3]Department of Human Genetics, Leiden University Medical Center, 2300 RC Leiden, Netherlands. [4]Department of Neurology, Leiden University Medical Center, 2333 ZA Leiden, Netherlands. [5]Department of Biochemistry and Molecular Pharmacology, NYU School of Medicine, New York, NY 10016, USA. [6]Perlmutter Cancer Center, NYU Langone Health, New York, NY 10016, USA. [7]Department of Neurology, Massachusetts General Hospital, Harvard Medical School, Boston, MA 02114, USA.
*Corresponding author. Email: sburden@mgh.harvard.edu (S.J.B.); rvanhauwaert@argenx.com (R.V.)
†These authors contributed equally to this work.
‡These authors contributed equally to this work.

and inducing postsynaptic differentiation. ARGX-119 is cross-reactive and specific for human, nonhuman primate (NHP), rat, and mouse MuSK. It has a nonlinear pharmacokinetic (PK) profile and rescues *Dok7* CM mice from early postnatal death and disease relapse in adult mice in a dose-dependent manner. These results support the translation of ARGX-119 to be tested in a clinical setting and illustrate the potential of a targeted therapy for treating neuromuscular diseases.

RESULTS

Generation of ARGX-119, a MuSK agonist antibody recognizing human, NHP, rat, and mouse MuSK

ARGX-119 is a humanized antibody derived from llamas that were immunized with the extracellular region of human MuSK (ECD) (fig. S1). ARGX-119 bound specifically to the Fz-like domain of human MuSK (Fig. 1A). The affinity and cross-species reactivity of ARGX-119 to human, NHP, rat, and mouse MuSK was quantified

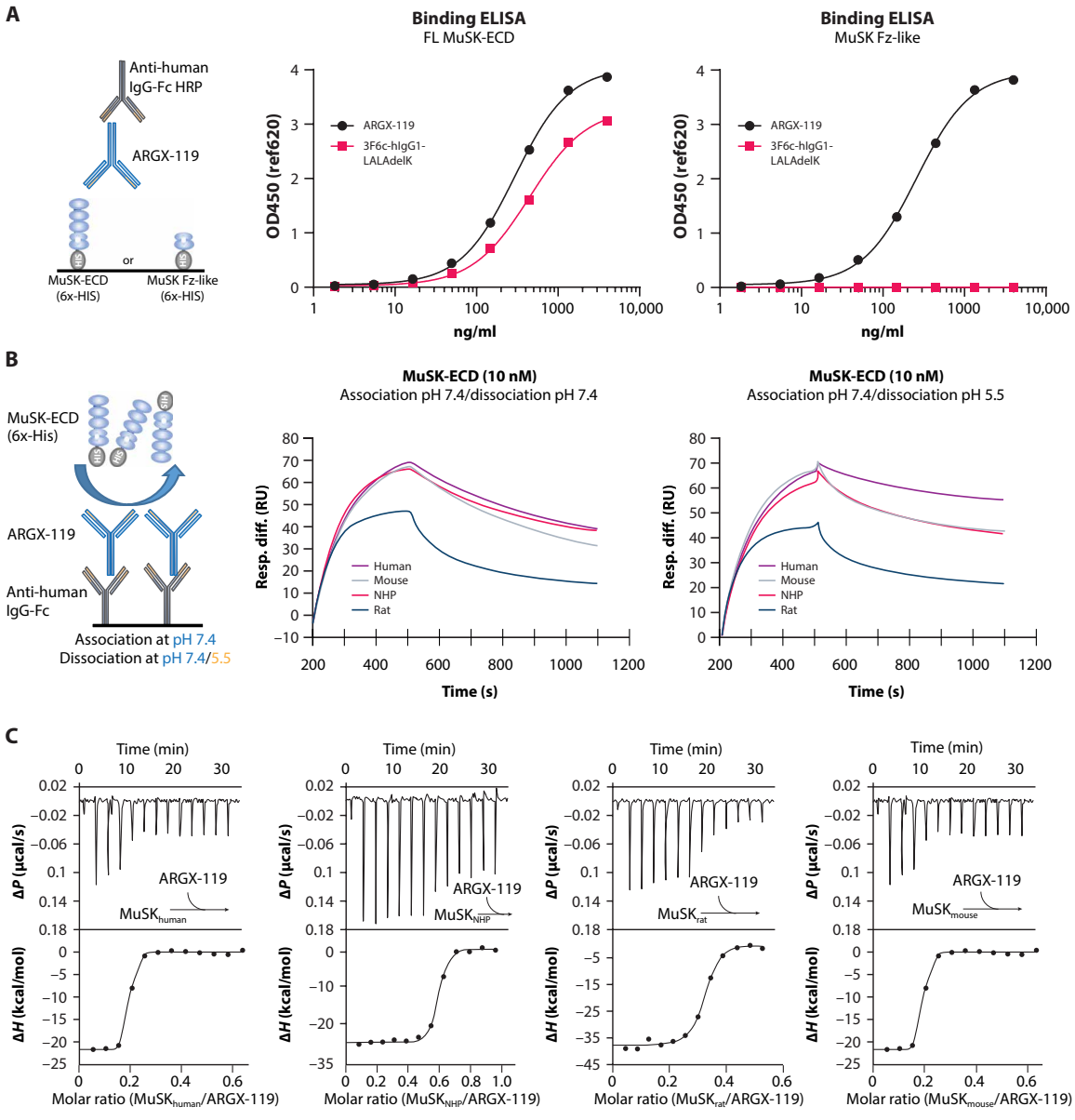

Fig. 1. ARGX-119, a MuSK agonist antibody recognizing human, NHP, rat, and mouse MuSK. (**A**) Cartoon illustrating the ELISA (left). Binding of ARGX-119 or a control antibody to the Ig1-like domain of MuSK (3F6c-hIgG1-LALAdelK), to MuSK-ECD (middle), or to MuSK Fz-like domain (right). OD, optical density. (**B**) Cartoon illustrating the binding of ARGX-119 to MuSK using SPR (left). A CM5 chip was coated with anti-human IgG-Fc, and ARGX-119 was captured at low densities. Sensorgrams show the binding kinetics of 10 nM human, NHP, mouse, and rat MuSK at a pH of 7.4 (middle) or 5.5 (right). RU, resonance units. (**C**) ITC experiment, investigating the binding thermodynamics of ARGX-119 to human, NHP, rat, and mouse MuSK in solution.

with surface plasmon resonance (SPR) and isothermal titration calorimetry (ITC) (Fig. 1, B and C; fig. S2, A to D; and table S1), which demonstrated that ARGX-119 binds MuSK across all species tested with similar affinities (K_d) and revealed no major pH-dependent dissociation.

ARGX-119 was formatted as a human IgG1 with L234A and L235A (LALA) mutations to reduce binding to Fc gamma receptors (FcγRs) and complement component 1q (C1q), diminishing Fc-mediated effector functions such as antibody-dependent cell-mediated cytotoxicity and complement-dependent cytotoxicity (*23*). ARGX-119 had little or no binding to human, NHP, rat, and mouse FcγRs. However, we detected a low but measurable affinity to the high-affinity human IgG-Fc receptor FcγRI (Table 1) (*24*, *25*). In addition, ARGX-119 showed strongly diminished binding to C1q across all species while retaining some reactivity to mouse C1q, as reported with other hIgG1-LALA antibodies (fig. S3, A to D) (*26*). These findings indicated that ARGX-119 had the anticipated characteristics; hence, IND (investigational new drug)–enabling studies were initiated.

ARGX-119 stimulates MuSK phosphorylation

We measured the ability of ARGX-119 to stimulate MuSK phosphorylation and AChR clustering in cultured myotubes from a human, NHP, rat, or mouse. ARGX-119 activated the MuSK pathway in a dose-dependent manner across all species tested (Fig. 2, A to E). ARGX-119 was more potent at inducing MuSK phosphorylation on human and NHP myotubes than on rodent myotubes (Fig. 2F and table S2). Similar results were found for the potency of ARGX-119 to induce AChR clustering (Fig. 2, G and H, fig. S4A, and table S2). Analysis of the AChR cluster size distribution revealed that the number and size of AChR clusters were comparable in mouse myotubes treated with Agrin or ARGX-119 (Fig. 2I).

In addition, MuSK phosphorylation in mouse and human myotubes was tested over a wide concentration range of ARGX-119. A bell-shaped dose-response curve, typical for receptor-dimerizing agonistic Abs (*27*), was observed over the concentrations tested (Fig. 3, A and B). Even at a high concentration of ARGX-119, Agrin (1 nM) could boost MuSK phosphorylation, indicating independent activation by ARGX-119 and Agrin (Fig. 3C). Likewise, at a low concentration of Agrin (0.1 nM), ARGX-119 acted cooperatively and increased MuSK phosphorylation beyond ARGX-119 or 0.1 nM Agrin alone (Fig. 3D). These findings indicate that ARGX-119 can activate MuSK independently from the natural activator Agrin, leading to increased MuSK phosphorylation.

Next, we investigated whether the reduced MuSK phosphorylation at high concentrations of ARGX-119 (without Agrin) affected AChR clustering. We tested a wide concentration range of ARGX-119 on mouse myotubes and found that ARGX-119 induced AChR clusters (>3 μm^2) at all ARGX-119 concentrations, reaching 80 to 100% of a saturating dose of neural Agrin (clusters of >3 μm^2 shown in Fig. 3, E and F; clusters of >15 μm^2 shown in fig. S4, A to C). These findings demonstrate that ARGX-119 is a potent activator of MuSK phosphorylation and AChR clustering in human, NHP, and rodent myotubes.

Table 1. ARGX-119 binding to FcγRs. ND, not detected.

FcγR		Averaged binding K_d (nM), $N = 3$		
		3B2g2m1-hIgG1-WTdelK	3B2g2m1-hIgG1-LALAdelK (ARGX-119)	3B2g2m1-hIgG1-LALAPGdelK
Human	hFcγRI	6.5	126.6	Low binding (>5000)
	hFcγRIIa 131H	780.0	Low binding (>5000)	ND
	hFcγRIIa 131R	1080.2	Low binding (>5000)	ND
	hFcγRIIb	Low binding (>5000)	ND	ND
	hFcγRIIIa 158F	1635.9	Low binding (>5000)	ND
	hFcγRIIIa 158V	344.8	Low binding (>5000)	ND
	hFcγRIIIb NA1	>5000	ND	ND
	hFcγRIIIb NA2	>5000	ND	ND
NHP	cFcγRI	10.6	Low binding (>5000)	Low binding (>5000)
	cFcγRIIa	2074.6	ND	ND
	cFcγRIIb	1422.7	Low binding (>5000)	ND
	cFcγRIII	127.6	Low binding (>5000)	ND
Mouse	mFcγRI	69.2	ND	ND
	mFcγRIIb	814.2	Low binding (>5000)	ND
	mFcγRIII	1028.7	Low binding (>5000)	ND
	mFcγRIV	392.2	Low binding (>5000)	ND
Rat	rFcγRI	316.5	Low binding (>5000)	Low binding (>5000)
	rFcγRIIa	ND	ND	ND
	rFcγRIIb	4960.4	Low binding (>5000)	ND
	rFcγRIII	470.9	Low binding (>5000)	ND

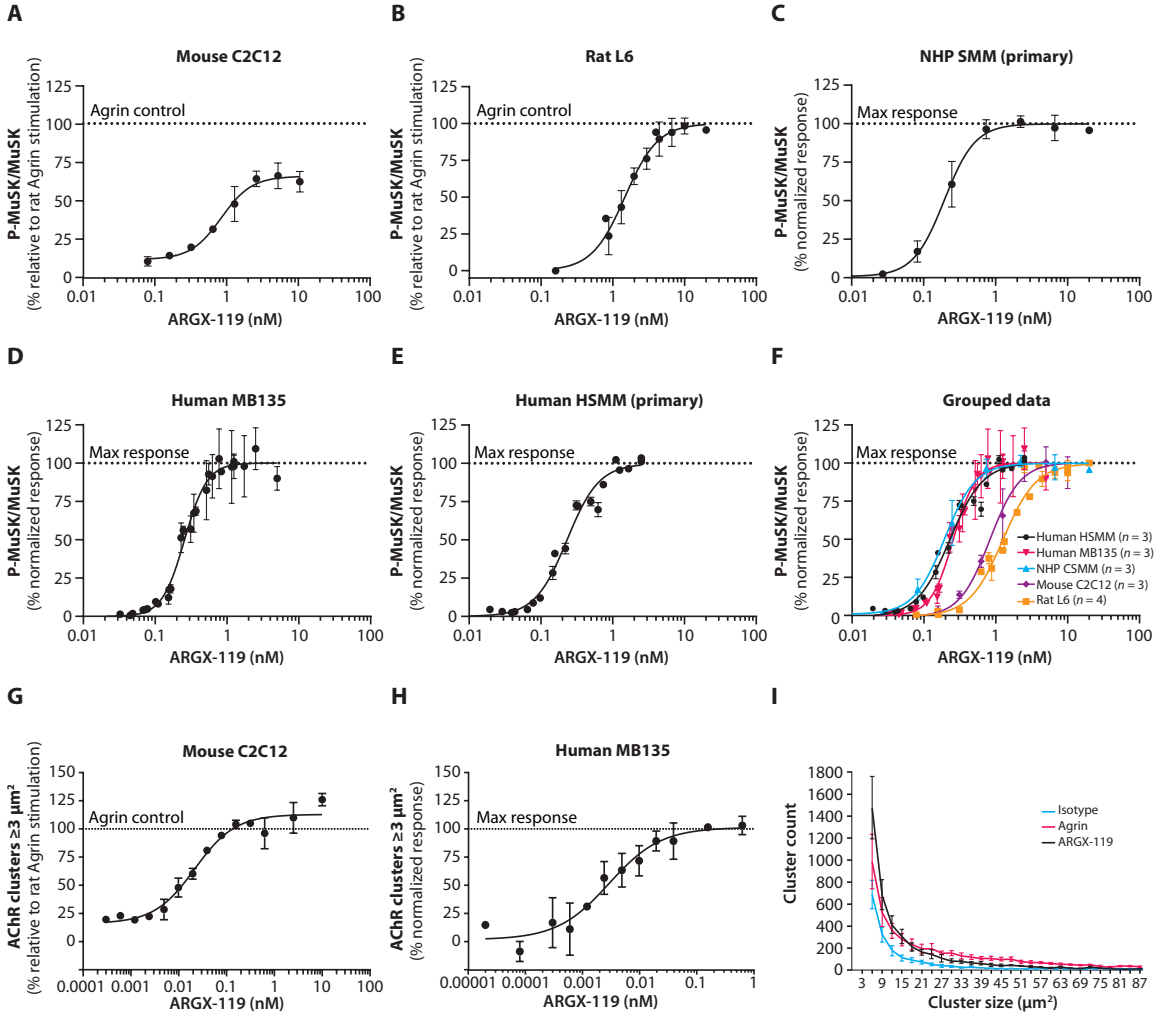

Fig. 2. ARGX-119 induces MuSK phosphorylation and AChR clusters in vitro across species. (**A** to **E**) MuSK phosphorylation normalized to total MuSK expression in (A) mouse C2C12, (B) rat L6, (C) NHP SMM primary, (D) human MB135, and (E) human HSMM primary myotubes treated for 30 min (mouse C2C12 treated for 10 min) with a dose range of ARGX-119. Data points are shown as means ± SD of at least three independent replicates ($N = 3$). (**F**) The graph shows the grouped data from (A) to (E). (**G** and **H**) Percentage of AChR clusters of ≥3 µm² in (G) mouse C2C12 relative to Agrin stimulation and (H) human MB135 myotubes relative to the maximal response, treated for 24 hours with a dose range of ARGX-119. (**I**) AChR cluster size distribution in C2C12 myotubes treated with Agrin, ARGX-119, or an isotype control antibody. AChR clustering data were generated from three independent experiments ($N = 3$). For reasons that are not fully understood, neural rat Agrin and neural human Agrin, produced in house, did not potently induce MuSK phosphorylation on human and NHP myotubes; therefore, the response was normalized to the maximal response (see Materials and Methods).

ARGX-119 binds specifically to MuSK

To assess potential off-target binding of ARGX-119, we used a plasma membrane protein array to measure binding of ARGX-119 to 5474 full-length human plasma membrane proteins and cell surface–tethered human secreted proteins plus 371 human heterodimers (*28*). ARGX-119 bound specifically to MuSK and failed to bind other proteins tested. In contrast, a previously described agonist antibody to MuSK, X17 (*17*), showed off-target binding to two other proteins (EphB1 and EphB2), making it unsuitable for clinical development (table S3).

ARGX-119 dosing in healthy mice reveals target saturation and target-mediated drug disposition

To determine whether ARGX-119 caused undesirable effects in wild-type mice, we repeatedly injected male and female mice intraperitoneally with ARGX-119 [10 mg/kg at postnatal days P4, P24, and P44 (Fig. 4, A to G) or twice a week (20 mg/kg) (fig. S5, A to H), beginning at P4]. As we reported previously for X17 and mab13, two different MuSK agonist antibodies targeting the Fz-like domain (*17*, *19*), chronic dosing of ARGX-119, using either dosing schedule, over 2 months had no effect on weight gain, motor behavior, the organization of NMJs, and survival when compared to wild-type mice injected with an isotype control Ab.

To gain insight into binding of ARGX-119 to MuSK at the NMJ, healthy wild-type adult mice were injected intraperitoneally once with ARGX-119 (0, 2, 10, or 20 mg/kg). Three days later, we visualized bound ARGX-119 by staining dissected muscles with fluorescently labeled antibodies to human Fc. ARGX-119 bound specifically to NMJs, marked by fluorescently labeled α-bungarotoxin (α-BGT) staining, in the diaphragm muscle in a dose-dependent

manner (Fig. 4, H and I). Statistical modeling based on these datasets estimated that 2.7% of MuSK was bound by an ARGX-119 dose of 0.125 mg/kg, 53% at 5 mg/kg, 70% at 10 mg/kg, and ~95% at 90 mg/kg (Fig. 4J). AChR expression, as determined by the α-BGT signal intensity, did not change in response to ARGX-119 (Fig. 4, H and K), indicating that MuSK phosphorylation was maximal at normally innervated NMJs, as described previously (*19*).

The PK of ARGX-119 was subsequently explored in single-dose studies with intravenous administration of 0.1 to 10 mg/kg to mice, 0.025 to 200 mg/kg to rats, and 0.25 to 100 mg/kg to NHPs (cynomolgus monkeys) (Fig. 5, A to C). These studies revealed a nonlinear PK behavior in all species, with PK parameters (exposure, clearance, and half-life) changing as a function of dose. Exposure (measured by the area under the curve) increased more than expected based on dose; clearance decreased and terminal secretion (half-life) increased with increasing dose (table S4). For an mAb, the most likely explanation for the nonlinear PK, as well as the observed shape of the time-concentration curves, is

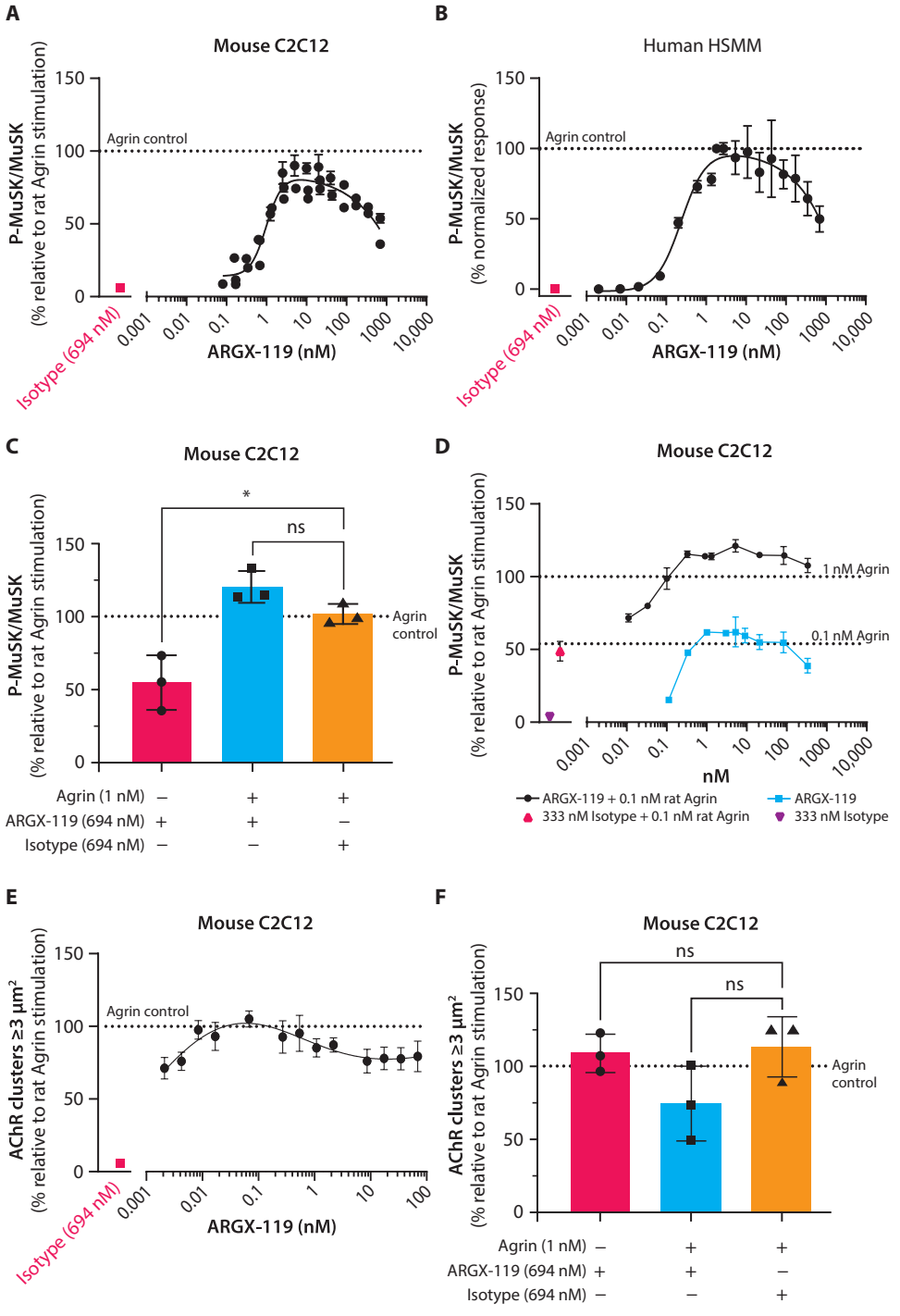

Fig. 3. ARGX-119 shows a bell-shaped dose-response curve and does not interfere with Agrin-induced MuSK phosphorylation and AChR clustering. (**A** and **B**) MuSK phosphorylation normalized to MuSK expression in (A) mouse C2C12 myotubes and (B) human HSMM primary myotubes treated for 30 min with a dose range of ARGX-119. Each data point represents the means ± SD of three independent experiments ($N = 3$). (**C**) MuSK phosphorylation normalized to total MuSK expression in mouse C2C12 myotubes treated with ARGX-119 (694 nM), ARGX-119 (694 nM) and Agrin (1 nM), or isotype control (694 nM) and Agrin (1 nM) ($N = 3$). (**D**) MuSK phosphorylation normalized to MuSK expression in mouse C2C12 myotubes treated for 30 min with a dose range of ARGX-119 and co-stimulated with 0.1 or 1 nM Agrin. Isotype controls are shown for comparison. Each data point represents the means ± SD of three independent experiments ($N = 3$). The dotted lines represent the 1 and 0.1 nM Agrin controls, resulting in 100 and 50% MuSK activation, respectively. (**E**) AChR clustering, showing the percentage of clusters of ≥3 µm² compared with Agrin controls in mouse C2C12 myotubes treated with a dose range of ARGX-119. (**F**) AChR clustering, showing clusters of ≥3 µm² in mouse C2C12 myotubes treated with Agrin, ARGX-119, isotype control mAb, or in combination. AChR clustering data were generated from three independent experiments ($N = 3$). One-way ANOVA with Dunnett's multiple comparisons (ns, not significant; *$P < 0.05$).

target-mediated drug disposition (TMDD), where the antibody binds to its target and is turned over together with the target. TMDD effectively adds an additional clearance to the nonspecific catabolic clearance that proteins undergo. Target binding is normally a saturable process; therefore, TMDD contributes to the overall clearance at low, nonsaturating doses. As doses increase and TMDD becomes saturated, the impact of TMDD decreases, and total clearance converges from the sum of TMDD and nonspecific catabolism to the lower value of nonsaturable catabolic clearance only. The presence of TMDD implies target binding; thus, it is indicative of in vivo target engagement. The terminal half-lives of ARGX-119 in healthy mice, at doses above saturation of TMDD, were, on average, 13 to 14 days for mice, 12 to 14 days for rats, and 17 days for cynomolgus monkeys. No differences in

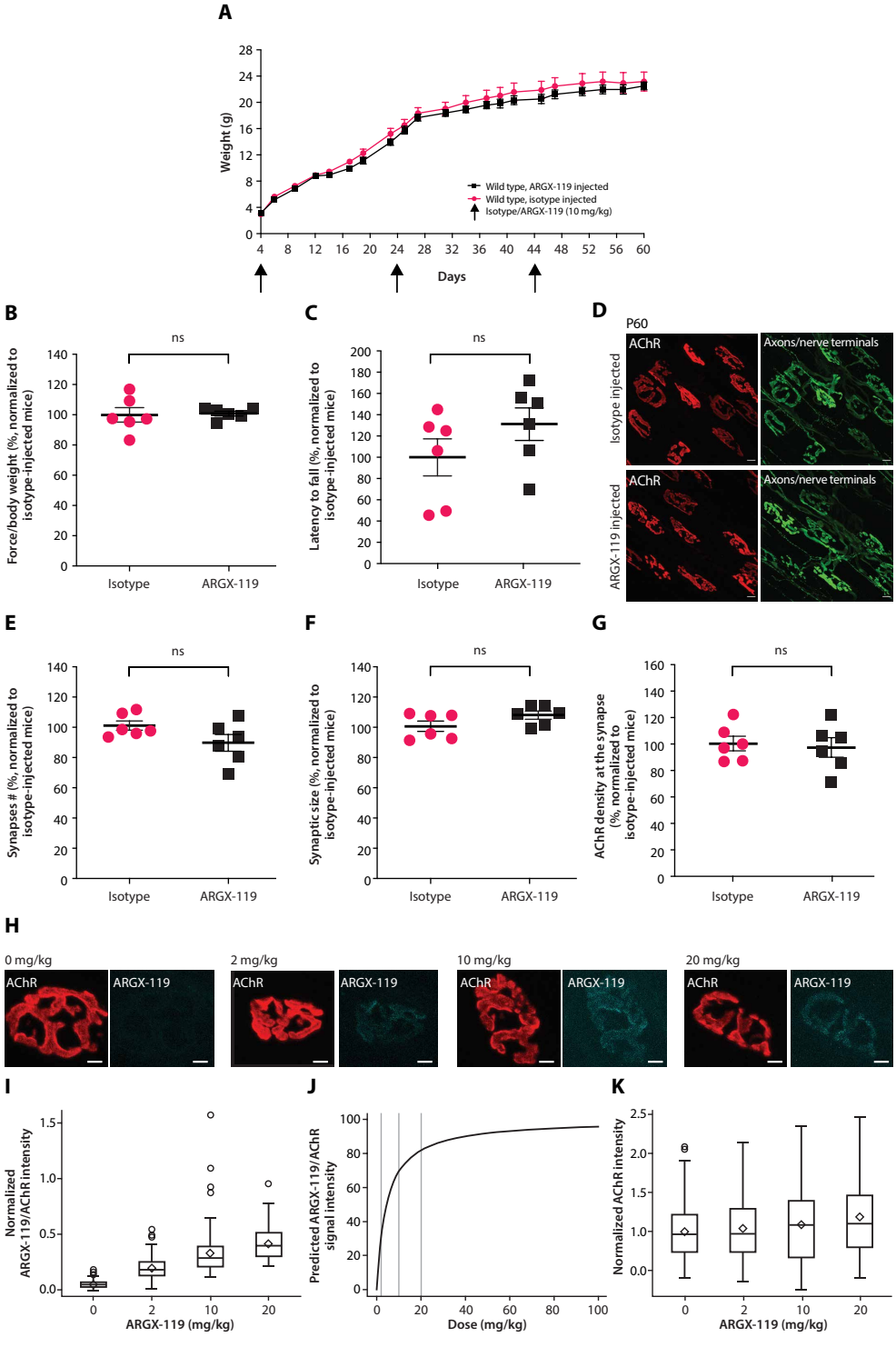

Fig. 4. ARGX-119 is specific for MuSK and binds to MuSK at NMJs in a dose-dependent manner. (**A**) Weights of wild-type mice injected with ARGX-119 or isotype control at P4, P24, and P44. Data are means ± SEM. (**B**) Grip strength quantified as force normalized to body weight of wild-type mice injected with ARGX-119 or isotype control at P60. (**C**) Latency to fall from a rotarod at P60 of wild-type mice treated as in (B). (**D**) Representative confocal images of synapses stained for AChRs, motor axons, and nerve terminals from 2-month-old (P60) wild-type mice treated with ARGX-119 or an isotype control antibody. Scale bars, 10 μm. (**E** to **G**) Number of synapses (E), synaptic size (F), and AChR density at synapses (G) of wild-type mice treated with ARGX-119 were normalized to wild-type mice injected with the isotype control antibody. Data points are shown as means ± SEM ($N = 6$ mice in each group). Two-sided Student's t test (ns, not significant). (**H**) Diaphragm muscles of P30 wild-type mice were stained for AChRs and human IgG (ARGX-119) 3 days after intraperitoneal injection of ARGX-119. Scale bars, 10 μm. (**I**) Box plot representation of ARGX-119/AChR intensity per ARGX-119 dosing group. (**J**) Graphical representation of the predicted ARGX-119/AChR signal intensities versus ARGX-119 dose (mg/kg). (**K**) Box plot representation of AChR intensity per ARGX-119 dosing group.

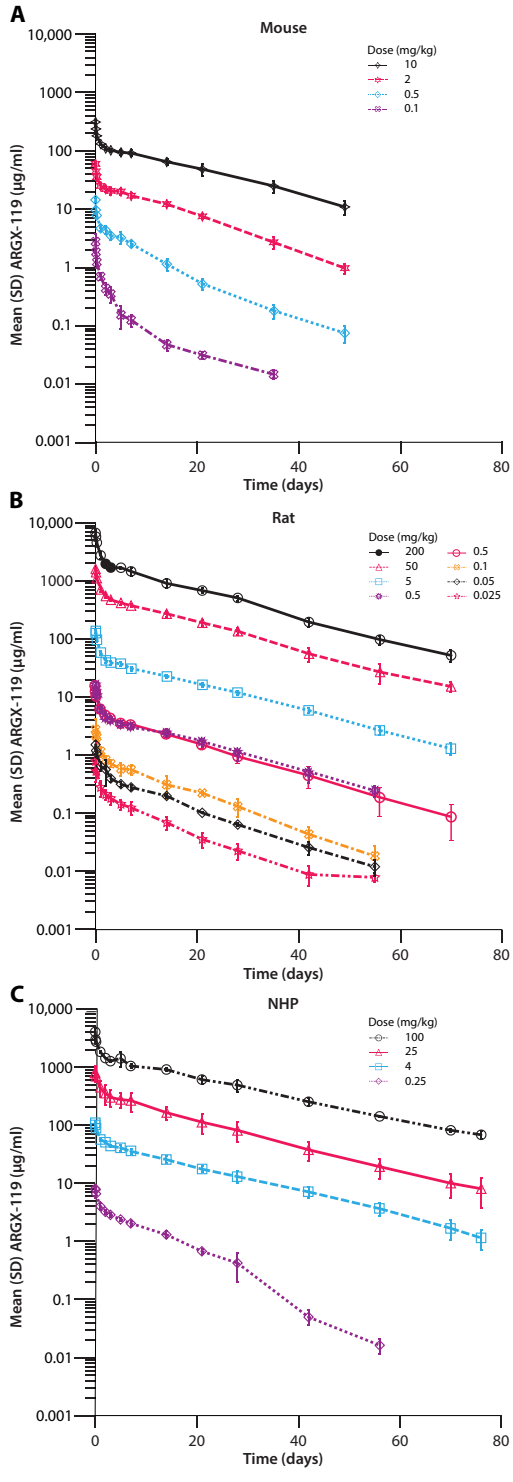

Fig. 5. ARGX-119 shows nonlinear PK behavior in NHPs, rats, and mice. (**A** to **C**) PK profile of ARGX-119 serum concentrations over time at different doses for (A) mice ($n = 12$ per dose), (B) rats ($n = 6$ per dose), and (C) NHPs ($n = 3$ per dose). Data are presented as means ± SEM.

PK parameters were observed between male and female animals (Fig. 5, A to C, and table S4).

ARGX-119 rescues neuromuscular synapse formation and prevents early postnatal lethality in *Dok7* CM mice in a dose-dependent manner

Dok7 CM mice harbor the most commonly found *DOK7* mutation in patients with *DOK7* CM, which truncates DOK7 and leads to impaired MuSK activation (*17*). *Dok7* CM mice display multiple deficits consistent with the human disease, including NMJ structural defects, muscle weakness, and fatigability (*15*, *17*). However, *Dok7* CM mice have a more severe disease presentation than humans with *DOK7* CM and die within 2 weeks after birth.

Dok7 CM mice were injected with ARGX-119 (20 mg/kg) at P4, followed by 10 mg/kg at P18 and P38. All *Dok7* CM mice treated with ARGX-119 ($N = 10$) survived until the end of the study (P60) and had normal muscle strength and fatigability at P60, whereas isotype control–treated *Dok7* CM mice ($N = 11$) died on average at P11 (fig. S6, A to D). The NMJs of the *Dok7* CM mice that were treated with ARGX-119 had a complex pretzel-like shape, which is characteristic of fully mature mouse NMJs, although the number and size of NMJs, as well as the density of synaptic AChRs, were not fully restored to normal (fig. S6, E to H).

To determine the minimal ARGX-119 dose needed to rescue the body weights and survival times of *Dok7* CM mice, a single dose of ARGX-119 was administered at P4, and body weight and survival were assessed. Eight ARGX-119 doses were tested, ranging from 0.125 up to 20 mg/kg (Fig. 6, A to I). An increase in body weight was observed in *Dok7* CM mice that received an ARGX-119 dose of 0.5 mg/kg or higher (Fig. 6J). In addition, time to body weight stagnation or loss and time to disease end point were also lengthened with an ARGX-119 dose of 0.5 mg/kg or higher (Fig. 6, K and L). These data suggest that a minimal ARGX-119 dose of 0.5 mg/kg at P4 is needed to improve the body weights and survival times of *Dok7* CM mice.

At ARGX-119 doses of 10 and 20 mg/kg, more substantial improvements in body weights and survival times were found. Most mice lived for more than 70 days after a single dose of ARGX-119 (Fig. 6, H to L). Therefore, a single ARGX-119 dose of 10 or 20 mg/kg at P4 was considered fully efficacious for the treatment of *Dok7* CM mice.

ARGX-119 reverses disease relapse in adult *Dok7* CM mice in a dose-dependent manner

We regularly monitored the body weights and muscle strength of *Dok7* CM mice injected with ARGX-119 (10 mg/kg) at P4. At a median of 68 days, *Dok7* CM mice began to lose weight and develop signs of muscle weakness. At relapse, the organization of NMJs had deteriorated (Fig. 7, A to D), and motor performance on a rotarod was diminished (Fig. 7, E and F). To determine the minimally active dose of ARGX-119 capable of reversing relapse in adult mice, a second dose of ARGX-119 (0.05 to 20 mg/kg) was administered at the time of disease relapse, defined as 5 consecutive days of weight loss. Survival, body weight, and muscle function were monitored for 28 days after the second dose (Fig. 8A). Relapsed mice treated with ARGX-119 gained weight within days, and their motor performance improved for at least 4 weeks. The minimally active dose range of ARGX-119 was 0.125 to 0.5 mg/kg. ARGX-119 doses from 2 to 20 mg/kg had a more consistent rescuing effect than lower doses; therefore, ARGX-119 doses

of 2 to 20 mg/kg were considered to be fully efficacious in this model (Fig. 8, B to E, and fig. S7, A to C).

Overall, these data suggest that ARGX-119 can rapidly reverse a progressive and lethal phenotype in a therapeutic setting in adult *Dok7* CM mice. Upon signs of body weight loss and muscle weakness, adult *Dok7* CM mice treated with ARGX-119 regained weight within days, and their motor performance improved for at least 4 weeks.

DISCUSSION

ARGX-119 is a recombinant mAb that binds specifically to the Fz-like domain of rodent, NHP (cynomolgus monkey), and human MuSK. The nonclinical data presented here were supportive for initiation of a phase 1a clinical trial investigating the effects of ARGX-119 in healthy volunteers (NCT05670704). ARGX-119 stimulated MuSK kinase activity and AChR clustering in a dose-dependent

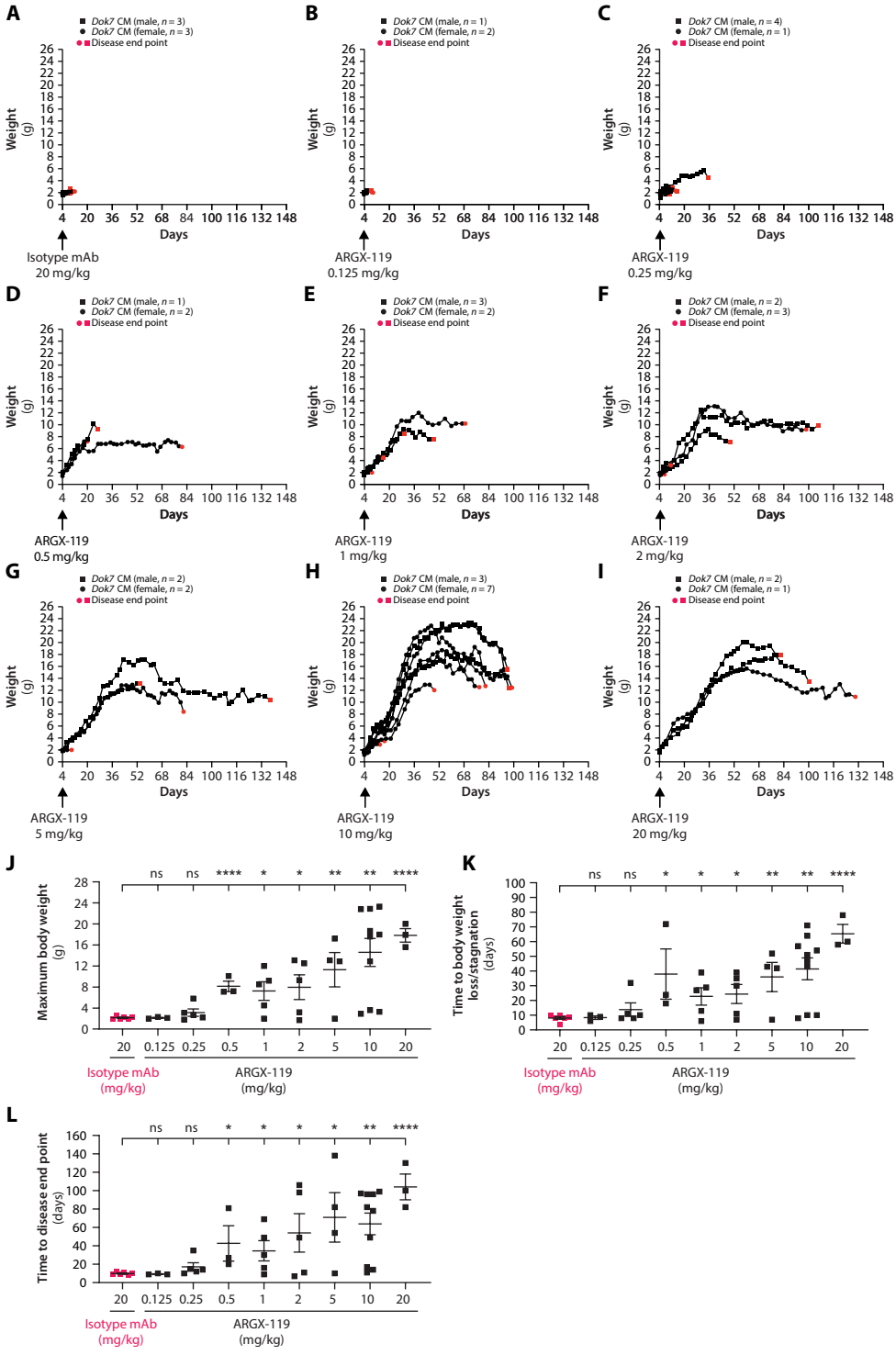

Fig. 6. ARGX-119 prevents early postnatal lethality of *Dok7* CM mice in a dose-dependent manner. (**A** to **I**) Body weights and survival times of *Dok7* CM mice after a single injection at P4 of an isotype control antibody at 20 mg/kg (A) or ARGX-119 at concentrations ranging from 0.125 to 20 mg/kg [(B) to (I)]. Red dots indicate disease end point, when the mice were euthanized (~20% weight loss) or died without severe signs of illness. Scatter plots show body weights for each *Dok7* CM mouse injected with ARGX-119 or the isotype control antibody. (**J** to **L**) Maximum body weight (J), time to body weight loss or stagnation (K), and time to disease end point (L) for mice treated with a dose range of ARGX-119. Scatter plots show individual data points and means ± SEM values ($n \geq 3$ mice for each group treated with the isotype control antibody or ARGX-119). Two-sided Student's *t* test (ns, not significant; $^{*}P < 0.05$; $^{**}P < 0.005$; $^{****}P < 0.00005$).

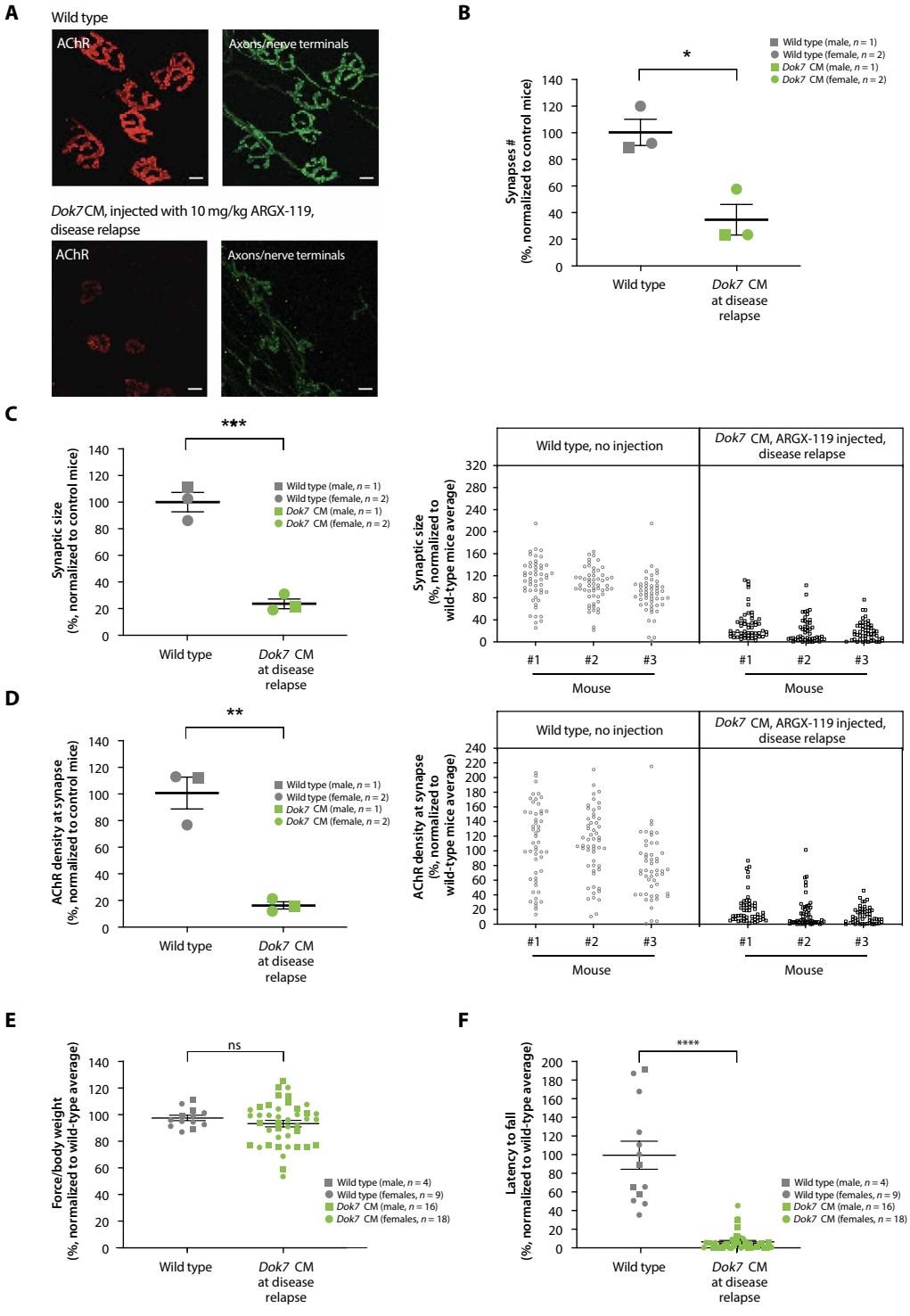

Fig. 7. The organization of the NMJ and muscle function deteriorates in *Dok7* CM mice at disease relapse. (**A**) Diaphragm muscles from wild-type mice (approximately P70) and *Dok7* CM mice at disease relapse were stained for AChRs and motor axons and nerve terminals. Scale bars, 10 μm. (**B**) Number of synapses for mice as in (A). (**C**) Average synaptic size (± SEM) (left) and individual synapse sizes (right) for *Dok7* CM mice at disease relapse and wild-type mice. (**D**) Average AChR density at the synapse (± SEM) (left) and AChR density for individual synapses (right) or mice as in (C). Two-sided Student's *t* test (ns, not significant; $*P < 0.05$; $**P < 0.005$; $***P < 0.0005$). (**E**) Grip strength quantified as force, normalized to body weights of wild-type mice (approximately P70) and *Dok7* CM mice at disease relapse. Scatter plots show the values for each mouse and mean as a percentage normalized to wild-type mice (average ± SEM). Two-sided Student's *t* test (ns, not significant). (**F**) Latency to fall from a rotarod at P60 of *Dok7* CM mice at disease relapse, as in (E) ($****P < 0.00005$).

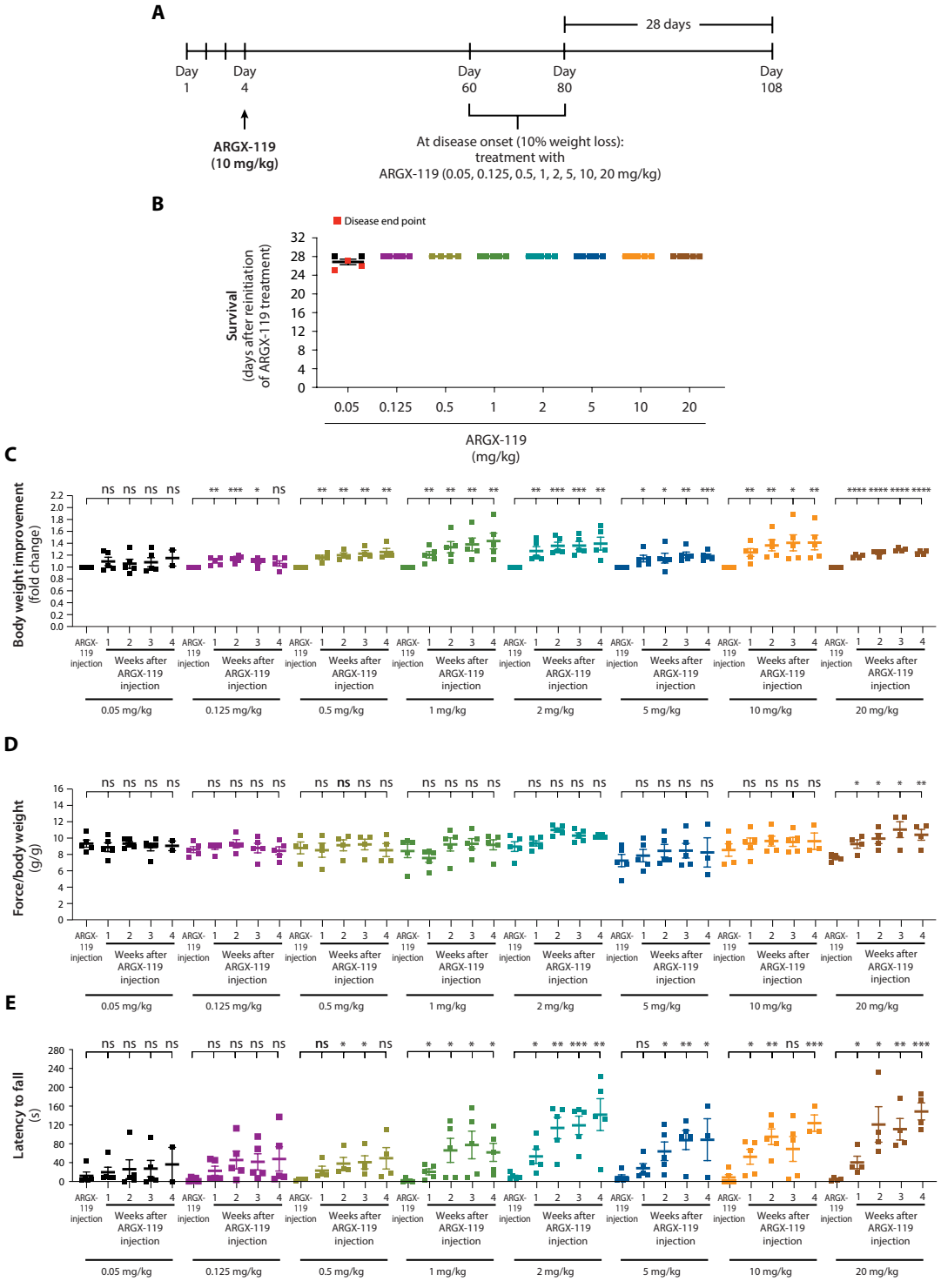

Fig. 8. ARGX-119 rescues disease relapse of *Dok7* CM mice in a dose-dependent manner. (**A**) Strategy to define the minimum dose of ARGX-119 to reverse disease relapse in adult *Dok7* CM mice. When *Dok7* CM mice had lost 10% of their body weight for 5 consecutive days, they were reinjected with a dose range of ARGX-119 (0.05 to 20 mg/kg) and monitored for 28 days. (**B**) Days of survival of *Dok7* CM mice retreated with ARGX-119 at doses described in (A). Experiments were terminated after 28 days. (**C**) Weight improvement of *Dok7* CM mice retreated with ARGX-119 at doses described in (A). Body weights (fold change) were normalized to body weight on injection day. Scatter plots show the values for each *Dok7* CM mouse injected with ARGX-119 and the means ± SEM. (**D**) Grip strength of mice after reinitiating ARGX-119 treatment at disease relapse at different doses. (**E**) Rotarod performances after reinitiating ARGX-119 treatment at disease relapse at different doses. Scatter plots show the values for each *Dok7* CM mouse injected with ARGX-119 and the means ± SEM values. $n \geq 3$ mice for each group dosed with the isotype control antibody or ARGX-119. Two-sided Student's *t* test (ns, not significant; $^{*}P < 0.05$; $^{**}P < 0.005$; $^{***}P < 0.0005$; $^{****}P < 0.00005$; s, seconds).

manner. The agonist antibody was well tolerated in mice given that the organization of neuromuscular synapses, muscle strength, and body weight were unperturbed in mice injected with ARGX-119 and no potential off-target antigens were identified. Previously described MuSK agonist Abs to the Fz-like domain either failed to bind human MuSK or bound off-target antigens, making these Abs unsuitable for clinical development.

ARGX-119 functions as a potent therapeutic in a mouse model of *DOK7* CM given that a single dose of ARGX-119 prevented early postnatal lethality and rapidly reversed disease relapse in adult *Dok7* CM mice. The prolonged rescue after a single injection of ARGX-119 may be due to the stability of the NMJ once formed, the high safety factor for synaptic transmission at the NMJ, a longer half-life of ARGX-119 in muscle tissue than in blood, or a combination of these factors. In any case, the potent and long-lasting benefit from ARGX-119 may allow for chronic dosing of ARGX-119 at monthly or longer intervals.

Together, these findings suggest that ARGX-119 may be a valuable therapeutic for *DOK7* CM and other neuromuscular diseases in humans. In mice, LRP4 expression and MuSK phosphorylation are reduced approximately twofold during aging, and boosting MuSK phosphorylation by *Dok7* overexpression increases synaptic size and synaptic transmission, leading to greater muscle strength and improved motor performance (*29*, *30*). Similarly, ARGX-119 has the potential to increase muscle strength and reduce sarcopenia during aging.

This study has limitations. Although the data presented here showed that ARGX-119 dose-dependently rescued a mouse model of *Dok7* CM, clinical trials will be needed to determine whether these findings translate to patients with *DOK7* CM.

Stimulating MuSK either with agonist antibodies to MuSK or by *DOK7* overexpression provides therapeutic benefit in mouse models of ALS, spinal muscular atrophy (SMA), and Emery-Dreifuss muscular dystrophy (*18*, *19*, *22*, *31*, *32*). Although the precise mechanisms by which boosting MuSK phosphorylation provides benefit in these disease models are not well understood, boosting MuSK phosphorylation stabilizes neuromuscular synapses that would otherwise deteriorate and disassemble in these diseases. Thus, ARGX-119 may provide therapeutic benefit on its own, or in combination with existing treatments, for neuromuscular diseases hallmarked by impaired neuromuscular synapses, including ALS and SMA.

MATERIALS AND METHODS

Study design

The purpose of this study was to generate and characterize an agonist mAb specific for a human, NHP, rat, and mouse Fz-like domain of MuSK that was suitable for clinical development. From llamas immunized with human MuSK, phage display selections, light chain shuffling, binding, and potency determinations, we identified ARGX-119. We investigated ARGX-119 binding to human, NHP, rat, and mouse MuSK, MuSK phosphorylation, and AChR clustering in human, NHP, rat, and mouse myotubes. We evaluated the binding of ARGX-119 to FcγRs and C1q. In addition, we assessed off-target binding using a plasma membrane protein array. We evaluated the body weight, muscle grip strength, and motor coordination by a rotarod, and we performed immunohistological analysis of synapses in diaphragm muscles from normal and ARGX-119–treated C57BL/6-CBA mice. Furthermore, we assessed the PK in cynomolgus NHPs, Wistar Han rats, and C57BL/6 mice. Last, we investigated whether ARGX-119 could rescue *Dok7* CM mice in a dose-dependent manner. This study did not use statistical methods for predetermination of sample size; the initial sample size was estimated from past experiments. The study was neither randomized nor blinded because of the severity of the model (early neonatal lethality). All experiments were performed in triplicate at minimum unless otherwise stated. No data were excluded.

Development of ARGX-119

Use of the SIMPLE (Superior Immunodiversity with Minimal Protein Lead Engineering) Antibody platform, which is based on the active immunization of outbred camelids (llamas) with target antigen, delivers antibodies whose variable regions are nearly identical to those of human antibodies. These variable domains are combined with human constant domains to generate full-size, fully human therapeutic antibodies. Here, llamas were immunized with recombinant human MuSK protein. RNA extraction was performed on peripheral blood lymphocytes isolated from the immunized llamas followed by reverse transcription polymerase chain reaction (PCR) and PCR cloning strategies to clone the llama Fab sequences in a phagemid as described previously (*33*). Panning phage display selections were performed after one/two or three rounds using either the extracellular domain of human or mouse MuSK or human MuSK lacking one or more Ig-like domains (fig. S1). Fz-like domain binding clones were enriched because this domain is not essential for MuSK function and is conserved across species (*21*). Moreover, antibodies against the Fz-like domain cause no obvious harm in mice, in contrast with Ig1-like domain binding antibodies (*17*–*19*, *34*). Individual clones were screened for binding to human and mouse MuSK by enzyme-linked immunosorbent assay (ELISA) but revealed poor human/mouse cross-reactive binding. Therefore, light chain shuffling was performed in an attempt to improve species cross-reactivity, and clones binding to both human and mouse MuSK were selected. These Fabs that bound MuSK were produced as human IgG1 antibodies (ImmunoPrecise Antibodies Ltd., Utrecht, Netherlands), containing the LALA mutations to reduce immune-activating effector functions. The terminal lysine of the heavy chain was removed to decrease heterogeneity. Potency of these antibodies was tested in a MuSK phosphorylation assay on mouse C2C12 myotubes and tested in vivo for rescue of early postnatal lethality of *Dok7* CM mice. Among several agonistic mAbs identified, specific clones were selected for further humanization by germ lining of its variable regions using genetic engineering to the framework regions of the closest human germ line with the highest identity (*33*).

SPR-based kinetic affinity measurements

The affinity of ARGX-119 for human, NHP (cynomolgus monkey), mouse, and rat MuSK was measured with a Biacore T200 SPR device (Cytiva). The immobilization buffer was 10 mM sodium acetate (pH 4.5), and the running buffer was HBS-EP+ (10 mM Hepes, 150 mM NaCl, and 3 mM EDTA) with 0.05% Tween 20 (pH 7.4). Goat anti-human IgG antibodies and the Fcγ fragment specific (109-005-098, Jackson Immunoresearch) were covalently immobilized onto all of the flow cells of a Sensor Chip CM5 Series S (Cytiva) at a high density using amine coupling chemistry. Next, ARGX-119 was captured, and one flow cell treated with the running buffer was used as a reference. MuSK proteins were then injected over the flow

cells using a twofold dilution series from 0.31 to 20 nM. Dissociation was evaluated using a running buffer at pH 7.4 or pH 5.5. Regeneration after every sample was carried out with an acid buffer [10 mM glycine HCl (pH 2.0)]. Analysis and calculation of binding data were carried out with the Biacore T200 evaluation software (version 3.2).

Binding thermodynamics

The thermodynamic footprint of ARGX-119 binding to the extracellular domain of human, NHP (cynomolgus monkey), mouse, and rat MuSK was determined by ITC on a MicroCal PEAQ-ITC Automated device (Malvern Panalytical). Proteins were thawed once at room temperature (RT) until a small amount of frozen solution remained, before placing the sample on ice to fully thaw. Both MuSK and ARGX-119 were diluted to appropriate working concentrations and dialyzed into 1× phosphate-buffered saline (PBS) (pH 7.4), using a Pur-A-Lyzer Midi Dialysis Kit (Sigma-Aldrich), before the start of experiments. Protein concentrations were confirmed using a NanoDrop spectrophotometer. All ITC experiments were carried out at 37°C using 3-μl injections spaced 150 s apart and preceded by a single 0.4-μl injection. Throughout the experiment, a stirring speed of 750 rpm was maintained. For each of the interactions, the affinities (K_d), apparent stoichiometries (n), enthalpy change (ΔH), entropy change (ΔS), and the Gibbs free binding energy (ΔG) were determined. Analyses were performed using the MicroCal PEAQ-ITC analysis software (Malvern Panalytical).

Data were analyzed using NITPIC (version 1.3.092,93) using the default parameters. Calculated heats and error estimates of all injections were transferred to Sedphat (version 1.294). Interactions were modeled using the "A + B + B ⇌ {AB} + B ⇌ ABB with two symmetric sites, macroscop K" model with the following global parameters: incfA = incfB = 0, not refined; Log(Ka1) = 6, refined; dHAB = −10, refined; Log10(Ka2/Ka1) macroscopic = −0.6, not refined; dH(AB)B-dHAB = 0, not refined. Under "experiment parameters," it was allowed to fit a baseline and estimate a local correction factor for the cell concentration. Buffer, pH, and temperature were completed, and given our setup, we selected "titrate A into B." After a global fit, the estimated thermodynamic parameters of the ABB reaction were calculated from those of the AB estimates. GUSSI (version 1.4.2) was used to generate a figure containing the thermogram and isotherms95. Representative ITC thermograms were selected and overlaid with the calculated thermodynamic parameters of the interactions.

MuSK-binding ELISA

Recombinant human MuSK ECD or the MuSK Fz-like domain was coated overnight at 4°C on a MaxiSorp plate (Thermo Fisher Scientific). The next day, the assay plate was blocked with a 1% casein blocking buffer (Bio-Rad) for 1 hour at RT. ARGX-119 and MuSK Ab 3F6c-hIgG1-LALAdelK [a MuSK MG patient–derived MuSK monoclonal targeting the Ig-like domain 1 of MuSK (*35*)] test dilutions were prepared fresh by diluting the stock solution in an assay buffer (0.1% casein in 1× PBS). These antibody dilutions were added in duplicate to the assay plate and incubated for 2 hours at RT. ARGX-119 was detected using a horseradish peroxidase–conjugated goat $F(ab')_2$ anti-human IgG-Fc polyclonal antibody (ab98741, Abcam) for 1 hour at RT followed by addition of the TMB (tetramethylbenzidine) substrate. The color development reaction was terminated by adding sulfuric acid, and the OD (optical density) at 450 nm was measured on an Infinite M Nano plate reader (Tecan). Results were processed using the GraphPad Prism 9.0 software.

MuSK phosphorylation assay

MuSK stimulation

MuSK phosphorylation was measured in myotubes. Myotubes were treated with ARGX-119 and Agrin with the indicated concentration for 30 min, unless stated otherwise. Recombinant neural rat Agrin (550-AG, R&D Systems) was included as a positive control using a saturating concentration of 1 nM. The isotype control (Mota-hIgG1-LALAdelK) was used at the same concentration as the highest applied concentration of ARGX-119. During the "high dose" experiments, ARGX-119 was serially diluted starting from as high as 694 nM. For the costimulation experiments of ARGX-119 with rat neural Agrin, a nonsaturating concentration of 0.1 nM Agrin, in combination with serial dilutions of ARGX-119 starting from 333 nM, was used. Cells were detached and lysed using the lysis buffer from a human phosphotyrosine MuSK ELISA kit (Item J, RayBiotech) supplemented with 2 mM activated sodium orthovanadate (Na_3VO_4) and protease and phosphatase inhibitor cocktails (Roche). Lysates could be stored at −80°C, but MuSK extraction was routinely immunoprecipitated immediately.

Extraction and detection of P-MuSK/MuSK on MSD

Immunoprecipitation of MuSK was initiated by adding biotinylated MuSK-Ig1 Ab 3F6c-hIgG1-LALAdelK to each of the lysates followed by an overnight incubation at 4°C. Bound antigen-antibody complexes were precipitated using streptavidin-coated magnetic beads (Promega) for at least 1 hour at 4°C, and the beads were washed extensively with the lysis buffer. MuSK proteins were eluted from the streptavidin-coated magnetic beads using 320 mM acetic acid (pH 2.6 to 2.7) followed by a neutralization step using 1 M Tris (pH 9.5).

Simultaneously, a streptavidin-coated MSD plate (Meso Scale Discovery) was blocked, and biotinylated MuSK-Ig1 Ab 3B5-hIgG4 was captured on the plate. MuSK, eluted from the streptavidin-coated magnetic beads, was loaded in quadruplicate on the plate, which allowed for detection of both total MuSK [by incubation with a mix of polyclonal MuSK Abs (PA1-1741, Thermo Fisher Scientific and MBS9205728, MyBioSource)] and tyrosine phosphorylated MuSK [by incubation with a mix of mouse anti-phosphotyrosine clone 4G10 (05-321, Millipore Corp.) and clone PY20 (ab10321, Abcam)] in the same sample in duplicate. Final detection occurred by applying SULFO-TAG–conjugated antibodies: anti-rabbit IgG for total MuSK detection (32AB-1, Meso Scale Discovery) and anti-mouse IgG for phosphorylated MuSK detection (R32AC-1, Meso Scale Discovery). Bound antibodies were detected through electrochemiluminescence using QuickPlex MSD (SQ 120, Meso Scale Discovery).

Analysis of P-MuSK/MuSK data

To compare datasets from different experiments performed on different days, a normalization step was performed. ARGX-119–induced MuSK phosphorylation was normalized to the Agrin-treated conditions for mouse C2C12 and rat L6 myotubes. For reasons that are not fully understood, neural rat Agrin and neural human Agrin produced in house did not potently induce MuSK phosphorylation on human and NHP (cynomolgus monkey) myotubes. These datasets were further normalized with the following formula: normalized response (%) = 100 × [(response − bottom)/(top − bottom)], where the bottom represents the isotype-treated signal and the top

represents the maximal signal. For the titration experiments, the normalized data were fit to a four-parameter nonlinear regression model using GraphPad Prism 9.0, from which the EC5, EC10, EC25, EC50, EC75, and EC95 concentrations were calculated. For the high-dose experiments, data were fit to a bell-shaped nonlinear regression model, and one-way analysis of variance (ANOVA) with Dunnett's multiple comparisons test was conducted to determine statistical significance using the GraphPad Prism 9.0 software. Last, for the Agrin costimulation experiments, data were normalized to the data for 1 nM Agrin and calculated using GraphPad Prism 9.0.

Stimulation and detection of AChR clusters

MuSK stimulation

Mature muscle myotubes had to be formed before AChR clustering experiments were initiated. All stimulations occurred for 24 hours unless stated otherwise. The stimulation times and test concentration range of ARGX-119 were optimized per cell line. Recombinant neural rat Agrin (R&D Systems) was always included as a positive control using a saturating concentration of 0.11 nM. The isotype control, Mota-hIgG1-LALAdelK, was always used at the highest applied concentration of ARGX-119. During the high-dose experiments, ARGX-119 was serially diluted starting from as high as 694 nM with and without costimulation of 1 nM Agrin.

Detection of AChR clusters

After 24 hours, mouse C2C12 myotubes were stained with Alexa Fluor 488–conjugated α-BGT (B13422, Thermo Fisher Scientific) and Hoechst (62249, Thermo Fisher Scientific) for 30 min and subsequently fixed with 4% paraformaldehyde (PFA) (JT Baker), washed, and stored in PBS at 4°C. Human MB135 cells were fixed with 4% PFA for 24 hours and sequentially stained with mAb35-mIgG2c produced and purified at Evitria SA, which binds AChRs (*36*), followed by a goat anti-mouse IgG secondary antibody conjugated to Alexa Fluor 488 (A32723, Invitrogen). Simultaneously with AChR staining, nuclei were stained with Hoechst, and the cells were washed and stored in PBS at 4°C. The plates containing the cells could be stored at 4°C for up to a week, but the plates were routinely analyzed within 24 hours. Imaging of AChR clusters was performed with an AF6000 fluorescence microscope (Leica AF6000) using a 20× objective. Five visual fields per well and four wells per condition were selected on the basis of evenly spread and visible mature myotubes in the bright-field channel.

Analysis of AChR clusters

Analysis of AChR clustering was performed using ImageJ (1.52n). We selected for AChR clusters in mouse C2C12 and human MB135 myotubes that were at least 3 μm^2 in size. ARGX-119–induced AChR clustering on mouse C2C12 myotubes was normalized to the number induced by rat neural Agrin. Because recombinant rat neural Agrin was not potent on MB135 human myotubes, we normalized the data as follows: expressed response (%) = 100 × [(response − bottom)/(top − bottom)], where the bottom represents the isotype-treated signal and the top represents the maximal signal. A one-way ANOVA with Dunnett's multiple comparisons test was used to determine statistical significance and was conducted using the GraphPad Prism 9.0 software.

Off-target binding

Off-target binding interactions of ARGX-119 and X17 (*17*) were assessed using the human plasma membrane protein cell array platform (Retrogenix Ltd., Chinley, United Kingdom). The antibodies were screened for binding against fixed human embryonic kidney (HEK) 293 cells individually expressing 5475 full-length human plasma membrane proteins and cell surface–tethered human secreted proteins plus 371 human heterodimers. Each library hit was reexpressed, along with two control receptors, and retested with test antibody or control treatments (1 μg/ml). This was performed both on fixed cells and on live cells in the absence of fixation. First, prescreens were undertaken to determine background binding of the test antibody to nontransfected HEK293 cells and cells overexpressing MuSK. These data were used to assess the suitability and optimal concentration for onward screening. Second, in the library screen, the test antibody was screened for binding against fixed HEK293 cells overexpressing 5475 individual full-length human plasma membrane proteins and cell surface–tethered human secreted proteins as well as a further 371 human heterodimers. Last, in the confirmation/specificity screens, all library hits were reexpressed and probed with the test antibody or control treatments to determine which hit(s), if any, was repeatable and specific to the test antibody. This was performed on both fixed and live cells.

Evaluation of wild-type C57BL/6-CBA mice

Injection of antibodies in C57BL/6-CBA mice

ARGX-119 was evaluated in healthy C57BL/6-CBA mice. C57BL/6-CBA mice were housed and maintained according to the Institutional Animal Care and Use Committee (IACUC) guidelines at NYU Medical School (IACUC ID no. IA16-00080). Mice received three intraperitoneal doses of 10 mg/kg at P4, P24, and P44 of either ARGX-119 ($n = 3$ males and $n = 3$ females) or an isotype control mAb ($n = 3$ males and $n = 3$ females). Alternatively, mice were intraperitoneally dosed twice per week, beginning at P5, with ARGX-119 (20 mg/kg) or an isotype control mAb until 60 days of age.

Body weight, muscle strength, and motor coordination measurements

Body weight was determined two times per week using an Ohaus PX2202/E Pioneer Precision Balance. Grip strength of male and female mice was measured using a grip strength apparatus (BIO-GS3, Bioseb) at P60 as described previously (*17*). To measure all-limb grip strength, mice were positioned in the center of a metal grid and held gently at the base of their tail. Mice were allowed to grip the grid with both forelimbs and hindlimbs, and they were pulled back steadily until the mice lost grip with the grid. The grip strength meter digitally displayed the maximum force applied (in grams) as the grasp was released. The means of six consecutive trials of all-limb measurements for each mouse were taken as an index of all-limb grip strength. Mice were given an interval of 10 to 15 s between trials. To enhance the robustness and reliability of the grip strength assessment, all measurements were taken by the same experimenter. Motor coordination of male and female mice at P60 was assessed on a rotarod (AccuRotor four-channel, Omnitech Electronics Inc.). Mice were placed on the rotarod (3.0-cm rotating cylinder) rotating at 2.5 rpm, and either the speed of rotation was increased linearly to 40 rpm over the course of 5 min or the speed of rotation was constant at 300 rpm. The time to fall from the rod was measured. Mice were subjected to three trials at 5-min intervals, and the longest latency to fall from the three trials was recorded. The two rotarod paradigms were done on the same day with a 1-hour time interval between paradigms. A Student's *t* test

was used to determine statistical significance and was analyzed using the GraphPad Prism 9 software.

Immunohistological analysis of diaphragm NMJs

Diaphragm muscles were dissected from P60 mice in an oxygenated L-15 medium. The muscles were pinned onto Sylgard-coated dissection dishes, fixed for 1.5 hours in 1% PFA, and blocked for 1 hour in PBT [PBS with 3% bovine serum albumin (BSA) (IgG-free, Sigma-Aldrich) and 0.5% Triton X-100]. Diaphragm muscles were stained with Alexa Fluor 488–conjugated α-BGT (Invitrogen) to label AChRs and with antibodies against β-TUBIII (302302, Synaptic Systems) or synapsin 1/2 (106002, Synaptic Systems) to label motor axons and nerve terminals, respectively. The antibodies were force pipetted into the muscle, and the muscles were incubated overnight at 4°C on an orbital shaker in a humidified chamber. Diaphragm muscles were washed 10 times over the course of 5 hours with PT (PBS with Triton X-100) at RT and rinsed in PBS before the muscle was whole-mounted in 50% glycerol. Images were acquired with a Zeiss LSM 800 confocal microscope using the ZEN software. Adjustments to detector gain and laser intensity were made to avoid saturation. The number and size of synapses as well as the density of synaptic AChRs were quantified using the FIJI/ImageJ software, as described previously (*37*). More than 50 synapses per diaphragm muscle from each mouse were quantified. A two-sided Student's *t* test was used to determine statistical significance and was conducted using GraphPad Prism 9.0.

Target engagement of ARGX-119 in C57BL/6-CBA mice

Injection of ARGX-119 in C57BL/6-CBA mice

Healthy male and female C57BL/6-CBA mice at postnatal day 30 were injected intraperitoneally with different doses (0, 2, 10, or 20 mg/kg) of ARGX-119. ARGX-119 was diluted in PBS before injection. There were three animals per dosing group: two males/one female in the 0 mg/kg group, one male/two females in the 2 mg/kg group, two males/one female in the 10 mg/kg group, and one male/two females in the 20 mg/kg group.

Immunohistological analysis of diaphragm NMJs

Three days after injection of ARGX-119, mice were euthanized, and diaphragm muscles were dissected in an oxygenated L-15 medium. The muscles were pinned onto Sylgard-coated dissection dishes, fixed for 1.5 hours in 1% PFA, and blocked for 1 hour in PBS with 3% BSA (IgG-free, Sigma-Aldrich) and 0.5% Triton X-100 (PBT). Diaphragm muscles were stained with Alexa Fluor 488–α-BGT to label AChRs (red) and Alexa Fluor 647 goat anti-human IgG, $F(ab')_2$ fragment specific to label ARGX-119 (cyan). ARGX-119 has an hIgG1-LALA-delK constant region, which can be detected specifically with the Alexa Fluor 647 goat anti-human IgG, $F(ab')_2$ antibody that is specific for detecting the Fab portion of human IgGs. Multiple images were acquired with a Zeiss LSM 800 confocal microscope and quantitated using ImageJ. Care was taken to ensure that the signal intensities were not saturating. Approximately 10 to 20 NMJs were imaged and quantitated (individual dots per image) from each image. Binding of ARGX-119 at the NMJ was measured by calculating the ratio of the signal intensity for ARGX-119 binding to the signal intensity for AChR expression.

Post hoc statistical analysis

The signal intensity data of all images from the 12 mice in the target engagement study were analyzed statistically. For each image, the background signal was quantitated for both AChR expression and ARGX-119 binding and subtracted from the respective total signal intensities. Evaluation of AChR expression in response to ARGX-119 was performed using a linear mixed model with restricted maximum likelihood in SAS Viya (v.03.04). The AChR signal intensities were normalized to the mean AChR signal intensity in the 0 mg/kg dose group and modeled in the function of ARGX-119 dose. Image number was included in the model as a random effect because it highly improved the model quality and random variability between images (and mice). The assumptions of normality and homoscedasticity of the residuals with expectation zero were confirmed. Wald hypothesis tests, with the Kenward-Roger approximation for the denominator degrees of freedom (*38*), were performed to compare the different doses, and *P* values were corrected by applying Hommel's procedure for multiple testing to control the family-wise error rate at 5%. The ratio of the ARGX-119 to AChR signal intensities, corrected for the background signal, was used to evaluate whether ARGX-119 binding to NMJs was dose dependent. The MCPMod (Multiple Comparison Procedure–Modelling) procedure was applied to evaluate the presence of a dose response. Dose-dependent binding of ARGX-119 to NMJs was confirmed and fitted with an E_{max} model, which is a monotone, concave dose-response model defined by three parameters: (i) E_0, the effect at a dose of 0 mg/kg; (ii) E_{max}, the maximum change asymptotically from 0 mg/kg; and (iii) ED_{50}, the half-maximal effective dose. The E_{max} model was used to predict the ratio of the ARGX-119 to AChR signal intensities, thus ARGX-119 binding to NMJs, as a function of dose. For graphical presentation, the predicted ARGX-119/AChR ratios from the E_{max} model were rescaled from 0 to 100% with 0 and 100% corresponding to the ratio at 0 mg/kg ARGX-119 ($= E_0$) and the maximal possible ratio predicted from the model ($= E_0 + E_{max}$). MCPMod was performed with R v4.0.1 using the package MCPMod.

PK study in NHPs, rats, and mice

The NHP study was performed at the Labcorp Harrogate site, according to UK animal welfare laws and under the supervision of the Labcorp animal welfare committee (license no. XE9A68DEA). Rat and mouse studies were performed at Charles River Laboratories France sites, according to the French animal welfare laws and under the supervision of Charles River Laboratories France under their license.

Six male and six female C57BL/6 mice per dose group were administered an intravenous bolus ARGX-119 dose of 0.1, 0.5, 2, or 10 mg/kg. Three male and three female Wistar [WI (Han)] rats per dose group received a single intravenous ARGX-119 infusion of 0.5, 5, 50, or 200 mg/kg over 1 hour. In a second study, four male Wistar [WI (Han)] rats per dose group received a single intravenous bolus ARGX-119 injection of 0.025, 0.05, 0.1, and 0.5 mg/kg.

Two male and one female NHP (cynomolgus monkey) per dose group received a single intravenous ARGX-119 infusion of 0.25, 4, 25, or 100 mg/kg over 20 min. Plasma or serum was collected at specified sampling times after dosing. Plasma or serum concentrations of ARGX-119 were determined by ELISA. Noncompartmental analysis was performed using Certara Phoenix WNL. Antidrug antibodies (ADAs) were not detected in mice; we detected ADAs in 4 of 40 rats and 1 of 12 cynomolgus monkeys. ADA-affected animals were excluded from analysis.

Mouse model for *Dok7* CM

The *Dok7* CM mouse model was first described in (*17*), and experiments described here were performed by the same person with the

same methods, using the same mouse strain (males and females). *Dok7* CM mice were housed and maintained according to the IACUC guidelines at NYU Medical School (IACUC ID no. IA16-00080). The isotype Ab used was Mota-hIgG1-LALAdelK. No statistical method was used to predetermine the sample size. No data were excluded from the analyses. The experiments were not randomized. The investigators were not blinded to the genotype of the mice with the exception of the motor performance experiments.

Supplementary Materials

The PDF file includes:
Methods
Figs. S1 to S7
Tables S1 to S4

Other Supplementary Material for this manuscript includes the following:
Data file S1
MDAR Reproducibility Checklist

REFERENCES AND NOTES

1. S. J. Burden, M. G. Huijbers, L. Remedio, Fundamental molecules and mechanisms for forming and maintaining neuromuscular synapses. *Int. J. Mol. Sci.* **19**, 490 (2018).
2. J. R. Sanes, J. W. Lichtman, Induction, assembly, maturation and maintenance of a postsynaptic apparatus. *Nat. Rev. Neurosci.* **2**, 791–805 (2001).
3. T. M. DeChiara, D. C. Bowen, D. M. Valenzuela, M. V. Simmons, W. T. Poueymirou, S. Thomas, E. Kinetz, D. L. Compton, E. Rojas, J. S. Park, C. Smith, P. S. DiStefano, D. J. Glass, S. J. Burden, G. D. Yancopoulos, The receptor tyrosine kinase MuSK is required for neuromuscular junction formation in vivo. *Cell* **85**, 501–512 (1996).
4. B. A. Hesser, O. Henschel, V. Witzemann, Synapse disassembly and formation of new synapses in postnatal muscle upon conditional inactivation of MuSK. *Mol. Cell. Neurosci.* **31**, 470–480 (2006).
5. D. M. Valenzuela, T. N. Stitt, P. S. DiStefano, E. Rojas, K. Mattsson, D. L. Compton, L. Nunez, J. S. Park, J. L. Stark, D. R. Gies, S. Thomas, M. M. le Beau, A. A. Fernald, N. G. Copeland, N. A. Jenkins, S. J. Burden, D. J. Glass, G. D. Yancopoulos, Receptor tyrosine kinase specific for the skeletal muscle lineage: Expression in embryonic muscle, at the neuromuscular junction, and after injury. *Neuron* **15**, 573–584 (1995).
6. R. Herbst, MuSk function during health and disease. *Neurosci. Lett.* **716**, 134676 (2020).
7. S. J. Burden, N. Yumoto, W. Zhang, The role of MuSK in synapse formation and neuromuscular disease. *Cold Spring Harb. Perspect. Biol.* **5**, a009167 (2013).
8. P. M. Rodriguez Cruz, J. Cossins, D. Beeson, A. Vincent, The neuromuscular junction in health and disease: Molecular mechanisms governing synaptic formation and homeostasis. *Front. Mol. Neurosci.* **13**, 610964 (2020).
9. D. J. Glass, D. C. Bowen, T. N. Stitt, C. Radziejewski, J. Bruno, T. E. Ryan, D. R. Gies, S. Shah, K. Mattsson, S. J. Burden, P. S. DiStefano, D. M. Valenzuela, T. M. DeChiara, G. D. Yancopoulos, Agrin acts via a MuSK receptor complex. *Cell* **85**, 513–523 (1996).
10. S. D. Weatherbee, K. V. Anderson, L. A. Niswander, LDL-receptor-related protein 4 is crucial for formation of the neuromuscular junction. *Development* **133**, 4993–5000 (2006).
11. B. Zhang, S. Luo, Q. Wang, T. Suzuki, W. C. Xiong, L. Mei, LRP4 serves as a coreceptor of agrin. *Neuron* **60**, 285–297 (2008).
12. W. Zhang, A. S. Coldefy, S. R. Hubbard, S. J. Burden, Agrin binds to the N-terminal region of Lrp4 protein and stimulates association between Lrp4 and the first immunoglobulin-like domain in muscle-specific kinase (MuSK). *J. Biol. Chem.* **286**, 40624–40630 (2011).
13. N. Kim, A. L. Stiegler, T. O. Cameron, P. T. Hallock, A. M. Gomez, J. H. Huang, S. R. Hubbard, M. L. Dustin, S. J. Burden, Lrp4 is a receptor for Agrin and forms a complex with MuSK. *Cell* **135**, 334–342 (2008).
14. K. Okada, A. Inoue, M. Okada, Y. Murata, S. Kakuta, T. Jigami, S. Kubo, H. Shiraishi, K. Eguchi, M. Motomura, T. Akiyama, Y. Iwakura, O. Higuchi, Y. Yamanashi, The muscle protein Dok-7 is essential for neuromuscular synaptogenesis. *Science* **312**, 1802–1805 (2006).
15. D. Beeson, O. Higuchi, J. Palace, J. Cossins, H. Spearman, S. Maxwell, J. Newsom-Davis, G. Burke, P. Fawcett, M. Motomura, J. S. Muller, H. Lochmuller, C. Slater, A. Vincent, Y. Yamanashi, Dok-7 mutations underlie a neuromuscular junction synaptopathy. *Science* **313**, 1975–1978 (2006).
16. N. Yumoto, N. Kim, S. J. Burden, Lrp4 is a retrograde signal for presynaptic differentiation at neuromuscular synapses. *Nature* **489**, 438–442 (2012).
17. J. Oury, W. Zhang, N. Leloup, A. Koide, A. D. Corrado, G. Ketavarapu, T. Hattori, S. Koide, S. J. Burden, Mechanism of disease and therapeutic rescue of Dok7 congenital myasthenia. *Nature* **595**, 404–408 (2021).
18. A. Sengupta-Ghosh, S. L. Dominguez, L. Xie, K. H. Barck, Z. Jiang, T. Earr, J. Imperio, L. Phu, H. G. Budayeva, D. S. Kirkpatrick, H. Cai, J. Eastham-Anderson, H. Ngu, O. Foreman, M. Hedehus, M. Reichelt, I. Hotzel, Y. Shang, R. A. D. Carano, G. Ayalon, A. Easton, Muscle specific kinase (MuSK) activation preserves neuromuscular junctions in the diaphragm but is not sufficient to provide a functional benefit in the SOD1(G93A) mouse model of ALS. *Neurobiol. Dis.* **124**, 340–352 (2019).
19. S. Cantor, W. Zhang, N. Delestree, L. Remedio, G. Z. Mentis, S. J. Burden, Preserving neuromuscular synapses in ALS by stimulating MuSK with a therapeutic agonist antibody. *eLife* **7**, (2018).
20. M. H. Xie, J. Yuan, C. Adams, A. Gurney, Direct demonstration of MuSK involvement in acetylcholine receptor clustering through identification of agonist ScFv. *Nat. Biotechnol.* **15**, 768–771 (1997).
21. L. Remedio, K. D. Gribble, J. K. Lee, N. Kim, P. T. Hallock, N. Delestree, G. Z. Mentis, R. C. Froemke, M. Granato, S. J. Burden, Diverging roles for Lrp4 and Wnt signaling in neuromuscular synapse development during evolution. *Genes Dev.* **30**, 1058–1069 (2016).
22. Z. Feng, S. Lam, E. S. Tenn, A. S. Ghosh, S. Cantor, W. Zhang, P. F. Yen, K. S. Chen, S. Burden, S. Paushkin, G. Ayalon, C. P. Ko, Activation of muscle-specific kinase (MuSK) reduces neuromuscular defects in the Delta7 mouse model of spinal muscular atrophy (SMA). *Int. J. Mol. Sci.* **22**, 8015 (2021).
23. M. S. Chappel, D. E. Isenman, M. Everett, Y. Y. Xu, K. J. Dorrington, M. H. Klein, Identification of the Fc gamma receptor class I binding site in human IgG through the use of recombinant IgG1/IgG2 hybrid and point-mutated antibodies. *Proc. Natl. Acad. Sci. U.S.A.* **88**, 9036–9040 (1991).
24. M. Brinkhaus, E. Pannecoucke, E. J. van der Kooi, A. E. H. Bentlage, N. I. L. Derksen, J. Andries, B. Balbino, M. Sips, P. Ulrichts, P. Verheesen, H. de Haard, T. Rispens, S. N. Savvides, G. Vidarsson, The Fab region of IgG impairs the internalization pathway of FcRn upon Fc engagement. *Nat. Commun.* **13**, 6073 (2022).
25. G. Dekkers, L. Treffers, R. Plomp, A. E. H. Bentlage, M. de Boer, C. A. M. Koeleman, S. N. Lissenberg-Thunnissen, R. Visser, M. Brouwer, J. Y. Mok, H. Matlung, T. K. van den Berg, W. J. E. van Esch, T. W. Kuijpers, D. Wouters, T. Rispens, M. Wuhrer, G. Vidarsson, Decoding the human immunoglobulin G-glycan repertoire reveals a spectrum of Fc-receptor- and complement-mediated-effector activities. *Front. Immunol.* **8**, 877 (2017).
26. I. Van de Walle, K. Silence, K. Budding, L. Van de Ven, K. Dijkxhoorn, E. de Zeeuw, C. Yildiz, S. Gabriels, J. M. Percier, J. Wildemann, J. Meeldijk, P. J. Simons, L. Boon, L. Cox, R. Holgate, R. Urbanus, H. G. Otten, J. H. W. Leusen, C. Blanchetot, H. de Haard, C. E. Hack, P. Boross, ARGX-117, a therapeutic complement inhibiting antibody targeting C2. *J. Allergy Clin. Immunol.* **147**, 1420–1429.e7 (2021).
27. P. A. Mayes, K. W. Hance, A. Hoos, The promise and challenges of immune agonist antibody development in cancer. *Nat. Rev. Drug Discov.* **17**, 509–527 (2018).
28. J. Freeth, J. Soden, New advances in cell microarray technology to expand applications in target deconvolution and off-target screening. *SLAS Discov.* **25**, 223–230 (2020).
29. R. Ueta, S. Sugita, Y. Minegishi, A. Shimotoyodome, N. Ota, N. Ogiso, T. Eguchi, Y. Yamanashi, DOK7 gene therapy enhances neuromuscular junction innervation and motor function in aged mice. *iScience* **23**, 101385 (2020).
30. K. Zhao, C. Shen, L. Li, H. Wu, G. Xing, Z. Dong, H. Jing, W. Chen, H. Zhang, Z. Tan, J. Pan, L. Xiong, H. Wang, W. Cui, X. D. Sun, S. Li, X. Huang, W. C. Xiong, L. Mei, Sarcoglycan alpha mitigates neuromuscular junction decline in aged mice by stabilizing LRP4. *J. Neurosci.* **38**, 8860–8873 (2018).
31. S. Arimura, T. Okada, T. Tezuka, T. Chiyo, Y. Kasahara, T. Yoshimura, M. Motomura, N. Yoshida, D. Beeson, S. Takeda, Y. Yamanashi, *DOK7* gene therapy benefits mouse models of diseases characterized by defects in the neuromuscular junction. *Science* **345**, 1505–1508 (2014).
32. M. Boido, E. De Amicis, V. Valsecchi, M. Trevisan, U. Ala, M. A. Ruegg, S. Hettwer, A. Vercelli, Increasing agrin function antagonizes muscle atrophy and motor impairment in spinal muscular atrophy. *Front. Cell. Neurosci.* **12**, 17 (2018).
33. H. J. de Haard, N. van Neer, A. Reurs, S. E. Hufton, R. C. Roovers, P. Henderikx, A. P. de Bruine, J. W. Arends, H. R. Hoogenboom, A large non-immunized human Fab fragment phage library that permits rapid isolation and kinetic analysis of high affinity antibodies. *J. Biol. Chem.* **274**, 18218–18230 (1999).
34. J. L. Lim, R. Augustinus, J. J. Plomp, K. Roya-Kouchaki, D. L. E. Vergoossen, Y. Fillie-Grijpma, J. Struijk, R. Thomas, D. Salvatori, C. Steyaert, C. Blanchetot, R. Vanhauwaert, K. Silence, S. M. van der Maarel, J. J. Verschuuren, M. G. Huijbers, Development and characterization of agonistic antibodies targeting the Ig-like 1 domain of MuSK. *Sci. Rep.* **13**, 7478 (2023).
35. M. G. Huijbers, D. L. Vergoossen, Y. E. Fillie-Grijpma, I. E. van Es, M. T. Koning, L. M. Slot, H. Veelken, J. J. Plomp, S. M. van der Maarel, J. J. Verschuuren, MuSK myasthenia gravis monoclonal antibodies: Valency dictates pathogenicity. *Neurol. Neuroimmunol. Neuroinflamm.* **6**, e547 (2019).
36. Y. F. Graus, M. H. de Baets, P. W. Parren, S. Berrih-Aknin, J. Wokke, P. J. van Breda Vriesman, D. R. Burton, Human anti-nicotinic acetylcholine receptor recombinant Fab fragments isolated from thymus-derived phage display libraries from myasthenia gravis patients reflect predominant specificities in serum and block the action of pathogenic serum antibodies. *J. Immunol.* **158**, 1919–1929 (1997).

37. A. Jaworski, S. J. Burden, Neuromuscular synapse formation in mice lacking motor neuron- and skeletal muscle-derived Neuregulin-1. *J. Neurosci.* **26**, 655–661 (2006).
38. M. G. Kenward, J. H. Roger, Small sample inference for fixed effects from restricted maximum likelihood. *Biometrics* **53**, 983–997 (1997).

Acknowledgments: We thank K. Moens, R. Coppejans, and L. De Clercq for experimental execution support, A. Van de Sompel for support with biostatistical analysis, E. Pannecoucke for contributing to the ITC experiments, S. Priem as the study monitor of the PK studies, and the argenx bioanalytical team (P. Vanhoenacker, L. De Cauwer, D. Defever, R. Tavares, and M. Notebaert) for support in assay development and sample analysis as well as J. Verschuuren and S. van der Maarel for the vibrant discussions. The LUMC forms part of the European Reference Network for Rare Neuromuscular Diseases (ERN EURO-NMD) and the Netherlands Neuromuscular Disorders Center (NL-NMD). **Funding:** This study was funded by argenx. M.G.H. receives support from a 2019 ZonMW VENI grant, LUMC Gisela Fellowship 2021, and the 2023 Dutch incentive grant. **Author contributions:** R.V., J.O., B.V., and S.J.B. supervised, assisted in the design and interpretation of experiments, and drafted the paper. C.S. conducted antibody selections using the SIMPLE Antibody platform, performed experiments, interpreted the data, contributed analysis tools, and critically revised the paper. S.M.J., D.L.E.V., C.K., L.S., J.L.L., J.J.P., and R.A. performed experiments, interpreted the data, and critically revised the paper. S.K., C.B., P.U., M.G.H., and K.S. supervised and assisted in the design and interpretation of experiments and critically revised the paper. **Competing interests:** R.V., B.V., C.S., C.K., J.L.L., C.B., P.U., and K.S. are (former) employees/consultants of argenx and are holders of employee equity in argenx. J.O., S.K., and S.J.B. are coinventors on MuSK-related (pending) patents. S.J.B. is a consultant for argenx. S.K. and S.J.B. have received research funding from argenx. M.G.H. and J.J.P. are coinventors on MuSK-related pending patents and receive royalties. LUMC receives royalties on a MuSK ELISA. M.G.H. received research funding from argenx and is a consultant for argenx. The other authors declare that they have no competing interests. **Issued patents:** Granted US Patent US 9,329,182 titled "Method of treating motor neuron disease with an antibody that agonizes musk," by applicant New York University with inventor S.J.B.; the pending EP and US Patent applications, derived from the international patent publication nr WO2020/055241 titled "MUSK activation," by applicant Academisch Ziekenhuis Leiden (h.o.d.n. LUMC) with inventors M.G.H. and J.J.P.; the pending EP and US patent applications, derived from the international patent publication nr WO2021/180676 titled "MUSK agonist antibody," by coapplicants argenx BV and Academisch Ziekenhuis Leiden with inventors C.B., C.S., D.L.E.V., M.G.H., and J.J.P.; granted US patent US 11,492,401 titled "Therapeutic musk antibodies," by coapplicants New York University and argenx BV, with pending counterparts in multiple jurisdictions, with inventors S.J.B., S.K., J.O., K.S., R.V., and C.B.; the pending patent family with the international patent publication number WO2023/147489 titled "Anti-musk antibodies for use in treating neuromuscular disorders," by coapplicants argenx BV, Université de Montréal, and New York University with inventors S.J.B., K.S., and R.V.; and the pending patent family with the international patent publication number WO2023/218099 titled "In utero treatment of a fetus having genetic disease/neuromuscular disease," by applicant argenx BV with inventors S.J.B., J.O., K.S., and R.V. **Data and materials availability:** All data associated with this study are present in the paper or the Supplementary Materials. ARGX-119 and other MuSK agonist antibodies can be provided to academic researchers upon request to the corresponding authors after completion of a material transfer agreement with argenx.

Submitted 17 February 2024
Resubmitted 29 April 2024
Accepted 26 August 2024
Published 18 September 2024
10.1126/scitranslmed.ado7189